Atomic-resolution structures from polycrystalline covalent organic frameworks crystals with enhanced Cryo-cRED

Jian Li
Peking University https://orcid.org/0000-0003-2221-2285
Cong Lin
Peking University https://orcid.org/0000-0003-0021-5055
Tianqiong Ma
Peking University https://orcid.org/0000-0002-5171-3209
Junliang Sun (junliang.sun@pku.edu.cn)
Peking University https://orcid.org/0000-0003-4074-0962

Article

Keywords:

Posted Date: May 5th, 2022

DOI: https://doi.org/10.21203/rs.3.rs-1609954/v1

Version of Record: A version of this preprint was published at Nature Communications on July 11th, 2022. See the published version at https://doi.org/10.1038/s41467-022-31524-9.

Abstract

The pursuit of atomic precision structure of porous covalent organic frameworks (COFs) is to understand relationship between structure and properties, and further develop new materials with superior performance. Yet, a challenge of how to determine their atomic structures has always existed since the first COFs was reported in seventeen years ago. Here, we presented a universal method for *ab initial* structure determination of polycrystalline 3D COFs at atomic level using enhanced cryo-cRED, which combined hierarchical cluster analysis with cryo-EM technique. The high-quality datasets are not only up to 0.79-angstrom resolution but more than 90% completeness, leading to unambiguous solution and precise anisotropic refinement. With such powerful method, the dynamics structures with flexible linkers, degree of interpenetration, position of functional groups, and arrangement of ordered guest molecules were successfully revealed with atomic precision in five 3D COFs, which were almost impossible to obtain these characteristics without atomic resolution structure solution. This study demonstrates a practicable strategy for determining the structures of polycrystalline COFs and other beam sensitive materials, and to help in the future discovery of novel materials on the other.

Introduction

Since the first covalent organic frameworks (COFs) was discovered as early as 2005 by Prof. Yaghi and co-worker[1,2], COFs are highly sought-after materials, which shown promising applications in molecule storage[3] and separation[4–8], heterogeneous catalysis[9–11], sensing[12–14], energy storage[15–17], optoelectronics[18], biomedical science[19,20], etc. Such diverse application strongly relied on the various structures and the kind of functional groups in COFs[21]. Over the past decade, a large number of COFs were obtained but most of their crystal structures were determined by analysis of powder X-ray diffraction data and aided by FTIR, solid state NMR spectroscopy and knowledge of reticular chemistry[22–26]. Due to the very low resolution of the PXRD data for the COFs materials, different research groups even interpreted as totally different topology with the same building block and PXRD[27,28]. Besides, without their precise structure at atomic level, many other uncertainties still remain: (i) inaccurate atomic positions and geometric parameters; (ii) uncertainties of degree of interpenetration and disorder in the frameworks; (iii) unknown guest arrangement; (iv) uncertainties configuration of functional group. Very few reported studies of COFs by single crystal X-ray diffraction (SCXRD) have proved that the precise atomic structure will help us to understand relationship between material structure and properties[29,30]. Due to the irreversible strong covalent bond properties, the COFs materials are always polycrystalline, which the structure revealing has been the key bottleneck for the COFs chemistry.

Three-dimensional electron diffraction (3DED) is an innovative technique developed as a complement to SCXRD for the structural elucidation of nanocrystals[31–33]. COF-320 is the first example that the structure was solved and refined by using rotation electron diffraction (RED, ~ 30min for data collection) data from nano single crystals in 2013[34]. Because of the beam damage, even cooling the crystals to 89K, the resolution of RED datasets of COF-320 were limited to 1.5 Å, preventing the ab initial structure

determination at the atomic level. Most of COF crystals can only survive for one to two minutes under the electron beam, the total angular coverage is ~ 60° with approximately 33.3% of the reciprocal space sampling volume using the advanced continuous mode of data collection, which resulted in limited completeness and redundancy of ~ 40% and ~ 0.5, respectively[35]. Although the 3D ED technique that we used have been reported for the structure solution of 3D COFs[18,36–42], it is far from routine and still a great challenge to obtain the atomic resolution of framework structure in COFs, let alone dynamics structures with flexible linkers, the determination of the degree of interpenetration, position of functional groups, arrangement of guest molecules, disorder in frameworks with atomic precision.

Herein, we demonstrate the enhanced Cryo-cRED method to address the beam damage issues of 3D COFs (Fig. 1). By combining hierarchical cluster analysis[43,44] with Cryo-EM technique, the 3DED data quality of resolution and completeness were improved significantly, which resulted in 0.79-angstrom resolution with more than 90% completeness. Using this method, structures of five complex 3D COFs (3D-TPB-COF-OMe, 3D-TPB-COF-Me, 3D-TPB-COF-OH, F-FCOF-5 and C-FCOF-5), including a series of 3D COF with different functional group, different degree of interpenetration and dynamic structure, were determined successfully at atomic level by the ab initial method. All the non-hydrogen atoms in the framework, together with the functional group and gust molecular, were located directly from the electrostatic potential map. Our achievement in this study represents a universal and superior method of ab initial structure determination of COFs at atomic level. It will definitely help us for better understanding the relationship between structure and property of COFs, and further develop new COFs with superior performance.

Results And Discussion

3D flexible COFs with dynamics structures. The applicability of enhanced Cryo-cRED was first demonstrated on a flexible 3D COF (FCOF-5), which is formed by the [4 + 4] imine condensation reaction between the molecules of 1,2,4,5-tetrakis[(4-formylphenoxy)methyl] benzene (TFMB) with flexible C-O single bonds in the backbone and the rigid tetra(*p*-aminophenyl)methane (TAPM) (Figure S1a, S2a and S3a). Due to the bond flexibility, this COF can undergo reversible structural expansion/contraction in response to guest molecular adsorption/desorption, indicating a breathing behavior. Although the simulated structures using PXRD were reported in our recent study[38], the dynamic structure at atomic level is still unknown. As the FCOF-5 is sensitive to the environment, the cRED sample preparation should be careful. For the sample preparation of expanded FCOF-5 (E-FCOF-5), a small quantity of micro-crystals was dispersed in ethanol by ultra-sonication for five minutes, and then a suspension droplet was transferred onto a copper grid covered with carbon film. From the grid, thousands of nano-crystals were easily discernible on the grid surface, providing ample nanocrystals for the 3DED data collection (Figure S4a). Prior to being transferred the grid into the transmission electron microscope (TEM), the sample was cooled to ~ 173 K using a cryo-transfer tomography holder to fix the guest molecules within the COF pores. After transferring the grid to electron microscopy, the sample was further cooled down to 96 K for 3DED data collection. To achieve high diffraction resolution, the spot size and exposure time were

optimized to 3 and 0.5 s, respectively. Although the E-FCOF-5 nano-crystals could diffract to a high resolution of ~ 0.82 Å, its crystallinity deteriorated quickly and the diffraction resolution dropped to ~ 3 Å at the final stage because of the serious beam damage (Figure S4-S5). From an individual dataset (dataset 1 in table S1), the unit cell parameters can be easily determined to be a = 14.58 Å, b = 8.51 Å, c = 26.49 Å, and β = 92.97° with monoclinic symmetry. The reflections conditions from specific slices were extracted as *h*0*l*: *l* = 2n, 00*l*: *l* = 2n, suggesting two possible space groups of *P*2/*c* (No. 13) or *Pc* (No.7) (Figure S5). Due to the completeness and redundancy were as low as 33% and 0.88 for an individual dataset, it failed to solve the E-FCOF-5 structure using ab initial method (direct method, charging flipping, etc.).

To improve the data completeness and redundancy for structure determination and refinement, the enhanced Cryo-cRED method, which is hierarchical cluster analysis[43,44] on several cryo-cRED datasets with different orientation of crystals. Twenty-two cRED datasets were collected on the E-FCOF-5 crystals with a large tilt range from 34.5^{o} to 95.2^{o} (detailed information of each dataset is listed in Table S1). The 3D reciprocal lattices reconstructed from the twenty-two datasets are shown in Figure S6, where the reciprocal lattice with a high resolution is in different locations owing to the different crystal orientations. Because E-FCOF-5 belongs to the monoclinic crystal system, none of the cRED datasets can have the completeness greater than 90%, which is necessary for a feasible structure refinement. Therefore, several datasets were carefully selected and merged. Before merging the data sets, all the cRED datasets were processed using an automated data procession method (Details are stated in Method Section). The twenty-two cRED datasets could be indexed with an average lattice parameters of *a* = 13.7095(2) Å, *b* = 8.633(6) Å, *c* = 26.4086(1) Å, and *β* = 91.393(2)°. The twenty-two datasets were then subjected to the hierarchical cluster analysis (HCA) using a python script developed in-house to determine the optimal datasets for merging[44]. The distance metric t, which defines the similarity between datasets, is derived from the correlation coefficients of the common reflection intensities (CC_I) in dataset pairs, and the "average" linkage method is employed. The clusters can be visualized using a dendrogram, making it easier to find an appropriate cut distance. Clusters with t < 0.40, in our experience with HCA, usually result in usable datasets. But in the E-FCOF-5 case, the distance metric value between each dataset is a little bit larger, which appears to be due to the beam damage. We thus cut the distance metric value with t = 0.5 to balance the completeness and obtained three clusters (Fig. 2a). The largest one (Fig. 2a, in red), consisting of sixteen datasets (Figure S6 and Table S1), possessed the highest data quality with the completeness and redundancy of 91% and 9.22, respectively. The sixteen data sets belonging to the largest cluster were merged. With such high-quality merged dataset (Fig. 2b), all non-hydrogen atoms were located directly from the electrostatic potential map by using ShelxT[45], resulting in a six-fold interpenetrated pts topology (Fig. 2f, Figure S7-left). Finally, the structure model was refined isotropically using soft restraints for the geometry of the phenyl ring as well as the C-C and C = N bond lengths. The guest molecular of ethanol can be determined by the difference electron density map (Fig. 2e), benefited from the high data completeness and resolution. With the atomic precision structure, the precise pore size of expanded FCOF-5 was obtained to be 6.2 Å×6.2Å and 4.2 Å×7.2Å (Fig. 2f), which was unknown in

previous study. (The details of cryo-cRED experimental parameters, crystallographic data, and structure refinement are in Table S2.)

For the contracted FCOF-5 (C-FCOF-5), the crystals were placed directly onto the copper grid without any dispersion. To ensure that the framework is fully contracted, the sample was transferred into the TEM with a high vacuum (< 2×10 − 5 Pa) at room temperature for five minutes to extract the guest molecules. After that, the sample was cooled to 96 K for data collection. Twenty-two cRED datasets (Table S3) were obtained on the C-FCOF-5 crystals, among which sixteen were selected for merging after HCA with the distance metric t of 0.56 (Fig. 2c, Figure S8). The C-FCOF-5 unit cell in the space group *P*2/*c* shrinks to *a* = 10.9511(2) Å, *b* = 7.7945(1) Å, *c* = 26.8214(6) Å, and β = 95.247(3)° (Figure S9) with a large volume contraction of ~ 27%, indicating a significant breathing motion. After similar data procession with E-FCOF-5, the completeness and redundancy for the C-FCOF-5 data were increased from 20 ~ 50% and ~ 1.0 (individual dataset) to 90% and 10.0 (merged sixteen datasets after HAC), respectively. The cRED data collected on the C-FCOF-5 crystals had a resolution of up to ~ 0.81 Å (Figure S10), and all the non-hydrogen atoms could be located directly from the electrostatic potential map using the ab initio structure solution with ShelxT[45], yielding the same six-fold interpenetrated pts topology with E-FCOF-5 (Fig. 2h, Figure S7-right). The C-FCOF-5 structure was also refined isotropically with soft restraints on the phenyl ring geometry as well as the C-C and C = N bond lengths and the observed peaks also appeared to be spherical with similar peak heights for the same atom types (Fig. 2g). As expected, the building block TFMB in the contracted FCOF-5 structure is twisted with its phenyl ring blocking the pores, thus no solvent void is accessible during the PLATON/SQUEEZE[46] procedure. From the atomic precision structure, the width was the pores of contracted FCOF-5 was only 1.7 Å (Fig. 2h), which finally revealed the reason of no N2 and Ar adsorption in our previous study. In addition, the bond angle and geometry of E-FCOF-5 and C-FCOF-5 that obtained from simulation of PXRD data shown a large deviation, comparing the atomic precision structure (Figure S11), atomic level structure determination is very important to understand the dynamics of flexible COFs. To our best knowledge, it is the first time that the structures of a flexible 3D COF at both the expansion and contraction states is resolved with atomic precision. (The details of cryo-cRED experimental parameters, crystallographic data, and structure refinement are in Table S4.)

3D COFs with functional group. The internal functional groups of 3D COF can be used to provide a structurally accurate application platform. Encouraged by the exciting results of FCOF-5, the applicability of enhanced cryo-cRED was employed on three 3D-TPB-COFs with different functional groups of methoxy (OMe), methyl (Me) and hydroxyl (OH), to thoroughly explore the scope and applicability of this powerful ab initial structure determination method. (Figure S1b, S2b, S3b-d). These three 3D-TPB-COFs were synthesized by the [4 + 4] condensation reaction of three 1,2,4,5-tetraphenylbenzene (TPB) derivatives, namely TPB-OMe, TPB-Me and TPB-OH functionalized by the respective methoxy, methyl and hydroxyl groups, with tetra(p-aminophenyl)methane (TAPM). The synthesis condition was described in our previous reports but the single crystal structures with atomic resolution are unclear[36,40,41].

For 3D-TPB-COF-OMe, the nano-crystals could diffract to a high resolution of ~ 0.87 Å at the beginning of the cryo-cRED[32,47] data collection (Figure S12), but the highest completeness and redundancy from a single dataset were ~ 65.9% and 1.55 (dataset 4# in table S5, Figure S13), respectively, resulting in missing observed peaks, significant variations in peak heights, and severe peak elongation during refinement (Figure S14). Eleven cRED datasets were collected on 3D-TPB-COF-OMe crystals (Table S5). The distance metric value is cut with $t = 0.3$, equivalent $CCI = 0.95$, which result in three clusters (Fig. 3b). The largest one consisting of six datasets (Fig. 3a), possessed the highest data quality with the completeness and redundancy of 91.8% and 8.43, respectively. With such high-quality merged dataset (Fig. 3c), all non-hydrogen atoms, including the functional group of OMe, were located directly from the electrostatic potential map by using ShelxT[45]. The structure refinement was greatly improved, from which the observed peaks appeared to be spherical with similar peak heights for the same atom types (Fig. 4a). The ordered guest molecular of water and ethanol in the pores of 3D-TPB-COF-OMe were observed at the final stage of refinement. In the end, the *R1* value was converged to 0.2281. With the same method, the atomic precession structure of 3D-TPB-COF-Me (Fig. 4b) and 3D-TPB-COF-OH (Fig. 4c) were determined directly and precise anisotropic refinement by merging 6 datasets (Table S7, Fig. 3d-3f, Figure S15-S16) and 4 datasets (Table S9, Figure S17-S19) after HAC, respectively. 3D-TPB-COF-OMe, 3D-TPB-COF-Me and 3D-TPB-COF-OH are determined to have a five-fold interpenetrated structure with a reported pts net with the same one-dimensional (1D) straight channels, but offering varied pore size (Fig. 4, Figure S20). In addition, the position of functional groups can be refined without any restraints. The obtained bond length of C-O(-C), (C=)C-C and (C=)C-O in methoxy, methyl and hydroxyl were 1.41Å, 1.55 Å and 1.28 Å, which close to the theoretical value (Fig. 4). (The details of cryo-cRED experimental parameters, crystallographic data, and structure refinement are in Table S6, S8 and S10, respectively.)

Discussion

In summary, we presented a powerful method for *ab initial* structure determination for sub-micron sized crystals of 3D COFs with Cryo-cRED data at the atomic level. The key study is the application of HCA, which contributes to the optimal selection of datasets for structure solution and refinement. And after merging the best-selected datasets, the quality regarding the data completeness and redundancy can be greatly improved. As proof of such a powerful method, five complex 3D COF structures were successfully solved at the atomic level using *ab initial* method, in which not only were all the non-hydrogen atoms in the framework located directly from the electrostatic potential map, but the dynamics structures with flexible linkers, degree of interpenetration, position of functional groups, arrangement of guest molecules were successfully revealed with atomic precision. Unlike other direct space methods for the 3D COF structure solution, the ab initial method does not require any knowledge of reticular chemistry. Although the emphasis of this study is on the 3D COF chemistry, the structure solution method mentioned here can also be applied for other beam sensitive materials, such as the small organic molecules, polymers, and organic-inorganic hybrid compounds.

Methods

Materials syntheses

Samples of the FCOF-5, 3D-TPB-COF-OMe, 3D-TPB-COF-Me and 3D-TPB-COF-OH were synthesized as described in previous reports[36,38,40,41].

TEM Sample preparation

For E-FCOF-5, 3D-TPB-COF-OMe, 3D-TPB-COF-Me and 3D-TPB-COF-OH TEM samples were prepared by firstly crushing the powder followed by dispersion in ethanol and ultrasonic treatment for five min. A drop of the dispersion was then deposited onto a 3 mm wide copper TEM grid covered by a carbon film. A high-tilt cryogenic sample holder (Gatan Company, Model 914) was used to freeze the sample to ~ 173 K before transferring the grid into TEM. The samples were further cooled to 96 K during data collection. For C-FCOF-5, the tiny crystals were loaded directly onto the copper grid without dispersion. To ensure that the framework is completely contracted, the sample is transferred into the TEM with high vacuum (< 2*10 − 5 Pa) at room temperature 5 min to remove the guest molecules, which was then cooled to 96 K for data collection.

3DED data collection

The continuous rotation electron diffraction (cRED) data were collected on the JEOL JEM-2100 transmission electron microscope (TEM, Cs: 1.0 mm, point resolution: 0.23 nm) at 200 kV using the instamatic script. During the data collection, the goniometer was rotated continuously while the selected-area ED patterns were captured from the individual crystal simultaneously by a quad hybrid pixel detector QTPX-262k (512 × 512 pixels with the size of 55 μm, Amsterdam Sci. Ins.). To track the crystals during data collection, the diffraction patterns were defocused at the interval of every 10 frames, and an image was taken with a short exposure (typically 0.01 s) to check the crystal position. The rotation speed of 0.45°/s and rotation step of 0.23° were used for each dataset, and all the ED patterns were recorded with the spot size of 3 and exposure time of 0.5 s.

Data procession

The 3D reciprocal lattice was reconstructed using the software REDp[47], which was powerful for indexing and obtaining the reflection conditions. Data processing was conducted using the software package XDS[48]. As a large number of cRED datasets need to be process, an automated data processing pipeline was used in this study, details of which can be found in our previous work. Shortly, the data processing pipeline consists of a set of Python scripts, including functions for automatically running XDS on all the datasets, extracting the lattice parameters and integration statistics, and cluster analyses. XDS is run for all the cRED dataset folders containing the file XDS.INP. If the dataset can be indexed successfully, the lattice parameters and integration statistics are then extracted from the file CORRECT.Lp. Then, hierarchical cluster analysis (HCA) is performed to find the most common unit cell using the lattice-based clustering method and to select the optimal datasets for merge using the reflection-based clustering method. XSCALE, one part of the XDS package, was used for merging the datasets and generating the hkl files that were used for structure solution and refinement.

Ab initial structure solution and refinement

The SHELX[49] software package was used for structural analysis, where SHELXT was used for structure solution and SHELXL for structure refinement. Atomic scattering factors for electrons based on the neutral atoms were used. All the atoms were refined anisotropically. DFIX constraints were used to maintain reasonable C-C and C-N distances during the refinement. PLATON/SQUEEZES[46] procedure was conducted to deduct the diffraction contribution from the disordered guest molecules within the pores at the final stage of refinement for 3D-TPB-COF-Me and 3D-TPB-COF-OH.

Data Availability

All the data supporting the findings of this study are available within the Article and its Supplementary Information, or from the corresponding author (J.S.) upon request. Crystallographic parameters for the structures are archived at the Cambridge Crystallographic Data Center (www.ccdc.cam.ac.uk/) under reference CCDC code: 2115021–2115025

Declarations

Acknowledgements

J.S. gratefull acknowledges financial support from the National Natural Science Foundation of China (U21A20285, 22125102, 21871009, 21527803), and J.L.thanks the Swedish Research Council (VR, grant No.1444205), the Knut and Alice Wallenberg Foundation (KAW, 2012-0112) through the 3DEM-NATUR project. Crystallographic parameters for the structures are archived at the Cambridge Crystallographic Data Center (www.ccdc.cam.ac.uk/) under reference CCDC code: 2115021-2115025. The authors thank Dr. Xiaoling Liu, Chao Gao, Yang Xie in Prof. Cheng Wang group (Wuhan university) provided the 3D COFs sample.

Author contributions

J.S. and J.L. designed the project. J.L. perfomred cRED experiment and solve the crystal structure. J.S. supervised the experiment. J.L., C.L., T.Q.M and J.S. prepared the manuscript draft and revised together.

Competing interests

The authors declare no competing interests.

Additional information

Supplementary information accompanies this paper can be found at https://www.nature.com/ncomms/.

References

1. Adrien P. Côté, A. I. Benin, Nathan W. Ockwig, Michael O'Keeffe, Adam J. Matzger, Omar M. Yaghi. Porous, Crystalline, Covalent Organic Frameworks. Science **310**, 1166–1170 (2005).
2. El-Kaderi, H. M.; Hunt, J. R.; Mendoza-Cortes, J. L.; Cote, A. P.; Taylor, R. E.; O'Keeffe, M.; Yaghi, O. M. Designed Synthesis of 3D Covalent Organic Frameworks. *science* **361**, 268–272 (2007).
3. Hiroyasu Furukawa, O. M. Y. Storage of Hydrogen, Methane, and Carbon Dioxide in Highly Porous Covalent Organic Frameworks for Clean Energy Applications.pdf. J. Am. Chem. Soc. **131**, 8875–8883 (2009).
4. Ma, H. *et al.* A 3D microporous covalent organic framework with exceedingly high C3H8/CH4 and C2 hydrocarbon/CH4 selectivity. Chem. Commun. **49**, 9773–9775 (2013).
5. Makhseed, S. & Samuel, J. Hydrogen adsorption in microporous organic framework polymer. Chem. Commun., 4342–4344 (2008).
6. Wang, C. *et al.* A 3D Covalent Organic Framework with Exceptionally High Iodine Capture Capability. Chemistry **24**, 585–589 (2018).
7. Fu, J. *et al.* Fabrication of COF-MOF Composite Membranes and Their Highly Selective Separation of H2/CO2. J. Am. Chem. Soc. **138**, 7673–7680 (2016).
8. Li, Z. *et al.* Three-Dimensional Ionic Covalent Organic Frameworks for Rapid, Reversible, and Selective Ion Exchange. J. Am. Chem. Soc. **139**, 17771–17774 (2017).
9. Fang, Q. *et al.* 3D microporous base-functionalized covalent organic frameworks for size-selective catalysis. Angew. Chem. Int. Ed. **53**, 2878–288 (2014).
10. Gonçalves, R. S. B. *et al.* Heterogeneous Catalysis by Covalent Organic Frameworks (COF): Pd(OAc)2@COF-300 in Cross-Coupling Reactions. ChemCatChem **8**, 743–750 (2016).
11. Li, H. *et al.* Three-Dimensional Covalent Organic Frameworks with Dual Linkages for Bifunctional Cascade Catalysis. J. Am. Chem. Soc. **138**, 14783–14788 (2016).
12. Li, Z., Zhang, Y., Xia, H., Mu, Y. & Liu, X. A robust and luminescent covalent organic framework as a highly sensitive and selective sensor for the detection of Cu^{2+} ions. Chem. Commun. **52**, 6613–6616 (2016).
13. Ding, S. Y. *et al.* Thioether-Based Fluorescent Covalent Organic Framework for Selective Detection and Facile Removal of Mercury(II). J. Am. Chem. Soc. **138**, 3031–3037 (2016).
14. Li, Z. *et al.* Light-Emitting Covalent Organic Frameworks: Fluorescence Improving via Pinpoint Surgery and Selective Switch-On Sensing of Anions. J. Am. Chem. Soc. **140**, 12374–12377 (2018).
15. Wu, C. *et al.* Highly Conjugated Three-Dimensional Covalent Organic Frameworks Based on Spirobifluorene for Perovskite Solar Cell Enhancement. J. Am. Chem. Soc. **140**, 10016–10024 (2018).
16. Lin, C. Y., Zhang, D., Zhao, Z. & Xia, Z. Covalent Organic Framework Electrocatalysts for Clean Energy Conversion. Adv. Mater. **30** (2018).

17. Zhang, Y., Riduan, S. N. & Wang, J. Redox Active Metal- and Covalent Organic Frameworks for Energy Storage: Balancing Porosity and Electrical Conductivity. Chemistry **23**, 16419–1643 (2017).
18. Ding, H. *et al.* An AIEgen-based 3D covalent organic framework for white light-emitting diodes. Nat. Commun. **9**, 5234 (2018).
19. Fang, Q. *et al.* 3D Porous Crystalline Polyimide Covalent Organic Frameworks for Drug Delivery. J. Am. Chem. Soc. **137**, 8352–8355 (2015).
20. Mal, A. *et al.* Supramolecular Reassembly of Self-Exfoliated Ionic Covalent Organic Nanosheets for Label-Free Detection of Double-Stranded DNA. Angew. Chem. Int. Ed. Engl **57**, 8443–8447 (2018).
21. Geng, K. *et al.* Covalent Organic Frameworks: Design, Synthesis, and Functions. Chem. Rev. **120**, 8814–8933 (2020).
22. Bunck, D. N. & Dichtel, W. R. Internal functionalization of three-dimensional covalent organic frameworks. *Angew. Chem. Int. Ed. Eng.l* **51**, 1885–1889 (2012).
23. Liu, Y. *et al.* 3D Covalent Organic Frameworks of Interlocking 1D Square Ribbons. J. Am. Chem. Soc. **141**, 677–683 (2019).
24. Lin, G. *et al.* 3D Porphyrin-Based Covalent Organic Frameworks. J. Am. Chem. Soc. **139**, 8705–8709 (2017).
25. Lin, G., Ding, H., Yuan, D., Wang, B. & Wang, C. A Pyrene-Based, Fluorescent Three-Dimensional Covalent Organic Framework. J. Am. Chem. Soc. **138**, 3302–3305 (2016).
26. El-Kaderi, H. M. *et al.* Designed synthesis of 3D covalent organic frameworks. Science **316**, 268–272 (2007).
27. Lan, Y. *et al.* Materials genomics methods for high-throughput construction of COFs and targeted synthesis. Nat. Commun. **9**, 5274 (2018).
28. Zhang, B. *et al.* Reticular Synthesis of Multinary Covalent Organic Frameworks. J. Am. Chem. Soc. **141**, 11420–11424 (2019).
29. Gropp, C., Ma, T., Hanikel, N. & Yaghi, O. M. Design of higher valency in covalent organic frameworks. Science **370** (2020).
30. Ma, T. K., E. A.; Yin, S.; Liang, L.; Zhou, Z.; Niu, J.; Li, L.; Wang, Y.; Su, J.; Li, J.; Wang, X.; Wang, W.; Wang, W.; Sun, J.; Yaghi, O. M. Single-crystal x-ray diffraction structures of covalent organic frameworks. Science **361**, 48–52 (2018).
31. Li, J. & Sun, J. Application of X-ray Diffraction and Electron Crystallography for Solving Complex Structure Problems. Acc. Chem. Res. **50**, 2737–2745 (2017).
32. Wang, Y. *et al.* Elucidation of the elusive structure and formula of the active pharmaceutical ingredient bismuth subgallate by continuous rotation electron diffraction. Chem. Commun. **53**, 7018–7021 (2017).
33. Yun, Y. *et al.* Phase identification and structure determination from multiphase crystalline powder samples by rotation electron diffraction. Journal of Applied Crystallography **47**, 2048–2054 (2014).

34. Zhang, Y. B. *et al.* Single-crystal structure of a covalent organic framework. J. Am. Chem. Soc. **135**, 16336–16339 (2013).
35. Ma, T. *et al.* Observation of Interpenetration Isomerism in Covalent Organic Frameworks. J. Am. Chem. Soc. **140**, 6763–6766 (2018).
36. Gao, C. *et al.* Isostructural Three-Dimensional Covalent Organic Frameworks. Angew. Chem. Int. Ed. **58**, 9770–9775 (2019).
37. Meng, Y. *et al.* 2D and 3D Porphyrinic Covalent Organic Frameworks: The Influence of Dimensionality on Functionality. Angew. Chem. Int. Ed. **59**, 3624–3629 (2020).
38. Liu, X. *et al.* A Crystalline Three-Dimensional Covalent Organic Framework with Flexible Building Blocks. J. Am. Chem. Soc. **143**, 2123–2129 (2021).
39. Sun, T., Wei, L., Chen, Y., Ma, Y. & Zhang, Y. B. Atomic-Level Characterization of Dynamics of a 3D Covalent Organic Framework by Cryo-Electron Diffraction Tomography. J. Am. Chem. Soc. **141**, 10962–10966 (2019).
40. Xie, Y. *et al.* Tuning the Topology of Three-Dimensional Covalent Organic Frameworks via Steric Control: From pts to Unprecedented ljh. J. Am. Chem. Soc. **143**, 7279–7284 (2021).
41. Gao, C., Li, J., Yin, S., Sun, J. & Wang, C. Redox-triggered switching in three-dimensional covalent organic frameworks. Nat. Commun. **11**, 4919 (2020).
42. Sun, T. *et al.* Direct-Space Structure Determination of Covalent Organic Frameworks from 3D Electron Diffraction Data. Angew. Chem. Int. Ed. **59**, 22638–22644 (2020).
43. Giordano, R., Leal, R. M., Bourenkov, G. P., McSweeney, S. & Popov, A. N. The application of hierarchical cluster analysis to the selection of isomorphous crystals. Acta Crystallogr D Biol Crystallogr **68**, 649–658 (2012).
44. Wang, B., Zou, X. & Smeets, S. Automated serial rotation electron diffraction combined with cluster analysis: an efficient multi-crystal workflow for structure determination. IUCrJ **6**, 854–867 (2019).
45. Sheldrick, G. M. SHELXT - integrated space-group and crystal-structure determination. Acta Crystallogr. A Found. Adv. **71**, 3–8 (2015).
46. Spek, A. L. Structure validation in chemical crystallography. Acta Crystallogr. D Biol. Crystallogr. **65**, 148–155 (2009).
47. Wan, W., Sun, J., Su, J., Hovmoller, S. & Zou, X. Three-dimensional rotation electron diffraction: software RED for automated data collection and data processing. J. Appl. Crystallogr. **46**, 1863–1873 (2013).
48. Kabsch, W. Integration, scaling, space-group assignment and post-refinement. Acta Crystallogr. D Biol. Crystallogr. **66**, 133–144 (2010).
49. Sheldrick, G. M. Phase Annealing in SHELX-90: Direct Methods for Larger Structures. Acta Cryst. **A46**, 467–473 (1990).

Figures

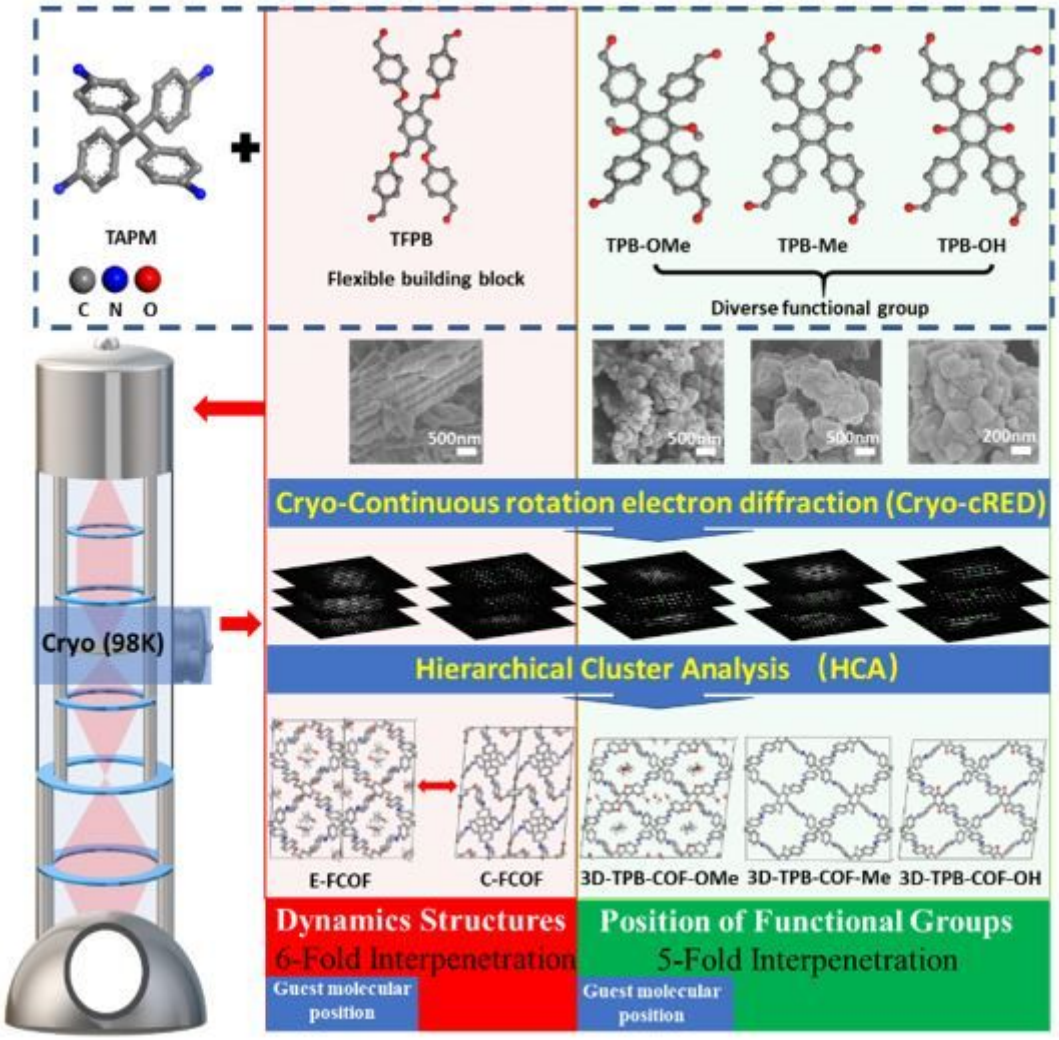

Figure 1

Chemical information of 3D COFs with flexible building block, different functional groups and the workflow of enhanced Cryo-cRED for the structure determination of polycrystalline COFs.

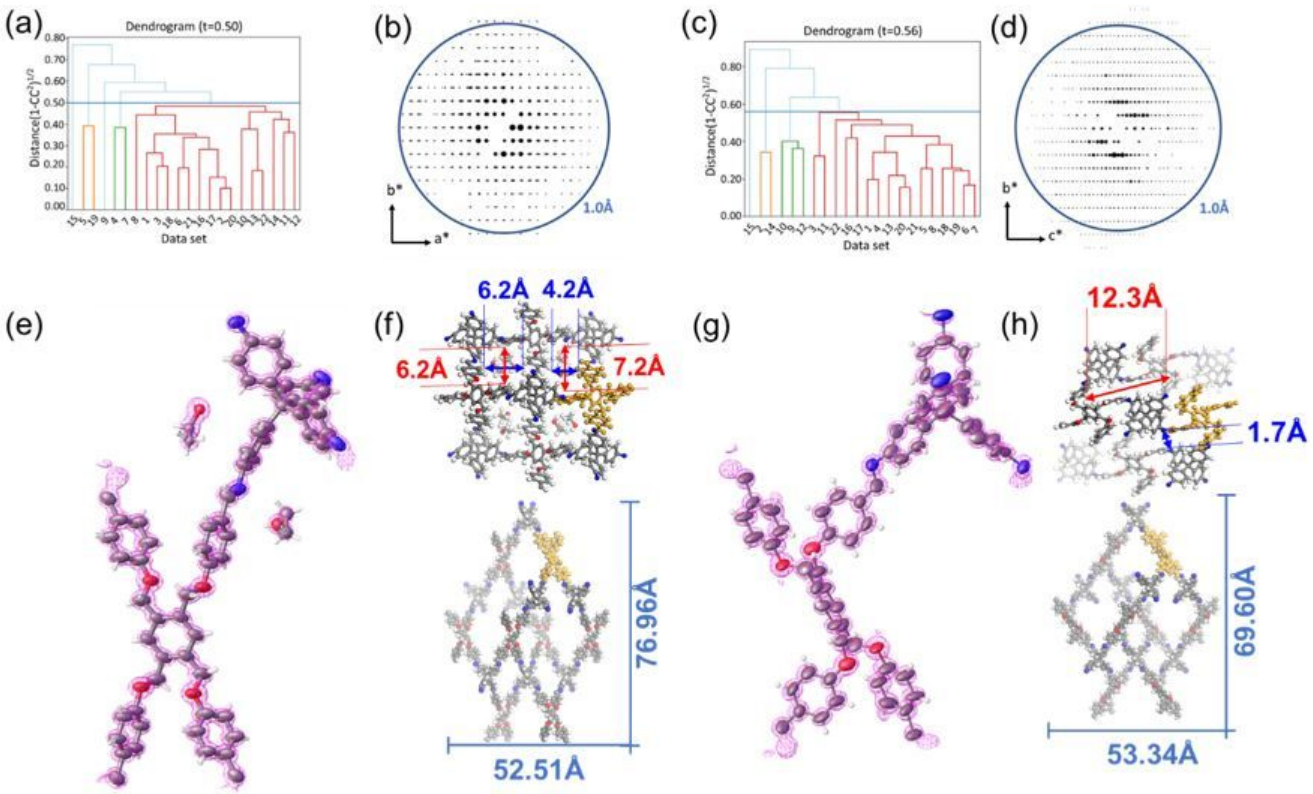

Figure 2

The cut distance of HCA is represented in dendrogram by the blue line at 0.5 for E-FCOF-5 (a) and 0.56 C-FCOF-5 (c), which resulted in 16 cRED datasets belongs to the largest cluster for E-FCOF-5 (a, in red) and E-FCOF-5 (c, in red). The overview of 3D reciprocal lattices of E-FCOF-5 (b) and C-FCOF-5 (d) that merging from 16 cRED datasets. The observed potential density maps of E-FCOF-5 (e) and C-FCOF-5 (g). The structures were refined isotropically using soft restraints for the geometry of the phenyl ring as well as the C-C and C=N bond lengths. The observed peaks appeared to be spherical with similar peak heights for the same atom types. The porous structure of E-FCOF-5 (f-up) and C-FCOF-5 (h-up). The single **pts** net of E-FCOF-5 (f-down) and C-FCOF-5 (h-down)

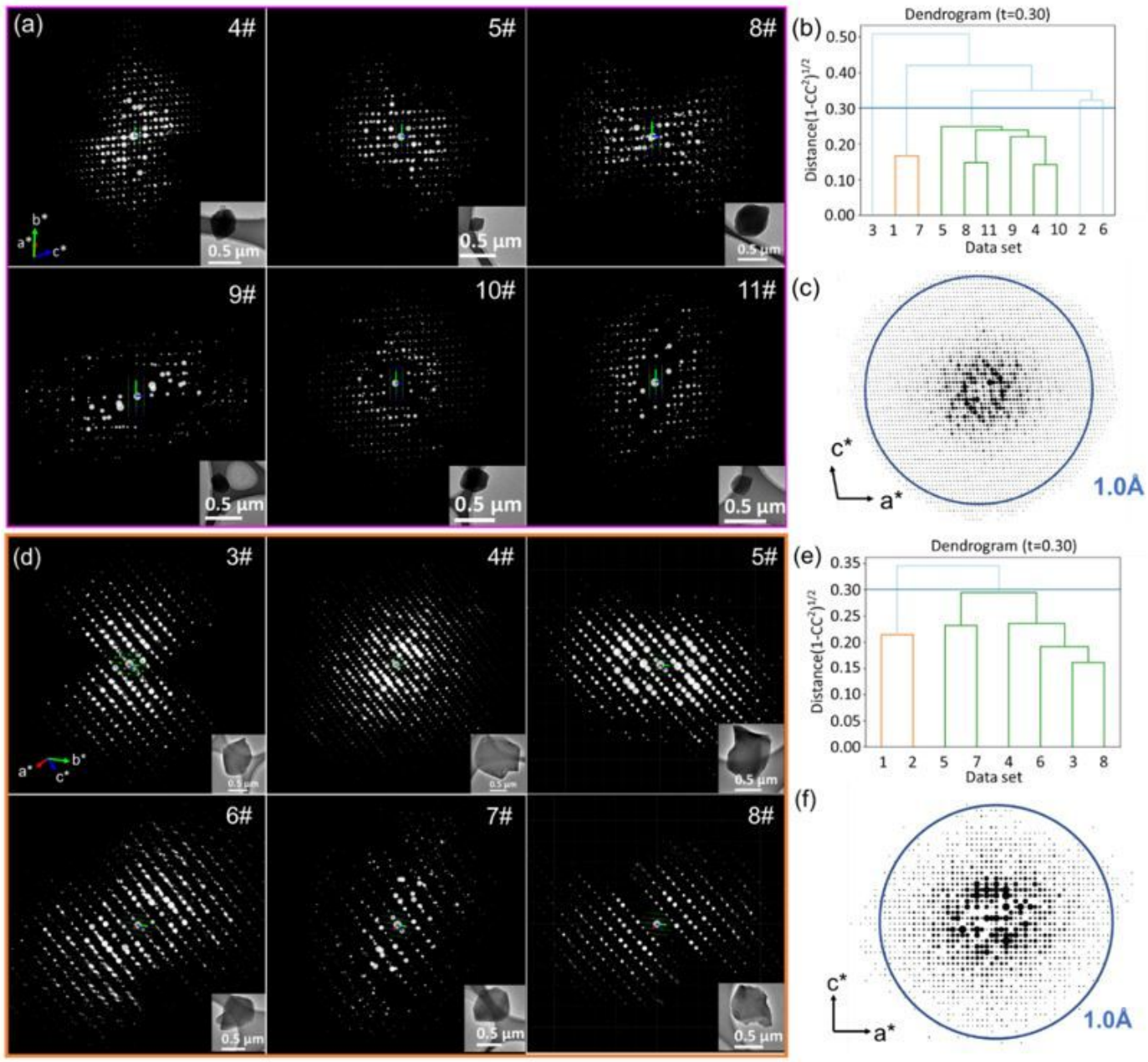

Figure 3

The overview of automatically selected six 3DED datasets of 3D-TPB-COF-OMe (a) and 3D-TPB-COF-Me (d) for merging and scaling. Dendrogram shows the results of the hierarchical cluster analysis (HCA) of extracted intensities, using the correlation coefficients of the common reflection intensities (CC_l) between pairs of datasets. The cut distance is represented by the blue line at 0.30 (corresponding to CC_l = 0.95) for 3D-TPB-COF-OMe (b) and 3D-TPB-COF-Me (e). In total, the largest clusters were identified with six cRED datasets for 3D-TPB-COF-OMe (b, in green) and 3D-TPB-COF-Me (e, in green), which were selected for the structure determination and refinement. The overview of merged 3D reciprocal lattices of 3D-TPB-COF-OMe (c), and 3D-TPB-COF-Me (f).

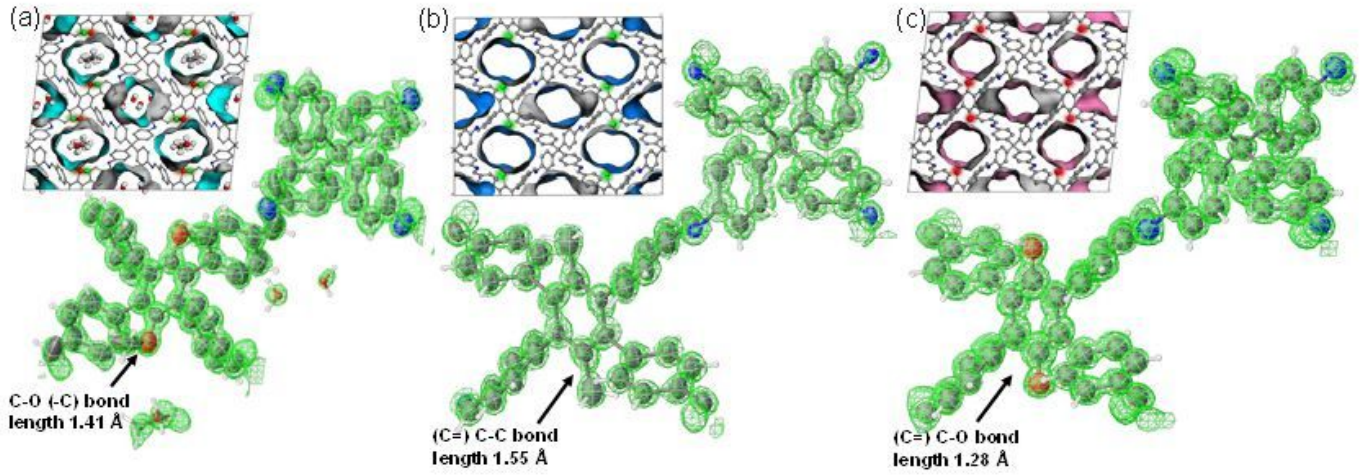

Figure 4

The observed potential density maps and crystal structures with 1D straight channels of 3D-TPB-COF-OMe (a), 3D-TPB-COF-Me (b) and 3D-TPB-COF-OH (c). Because of high resolution, high completeness of the dataset after HCA, not only the framework atoms can be located directly, but also the functional group and guest molecular can be determined with atomic precision by *ab initial* method. Color scheme: C in the framework, gray; O, red; N, blue; C in the functional group, green.

Supplementary Files

This is a list of supplementary files associated with this preprint. Click to download.

- CFCOF5.cif
- COF0429SI.docx
- 3DTPBCOFOMe.cif
- EFCOF5.cif
- 3DTPBCOFOH.cif
- 3DTPBCOFMe.cif